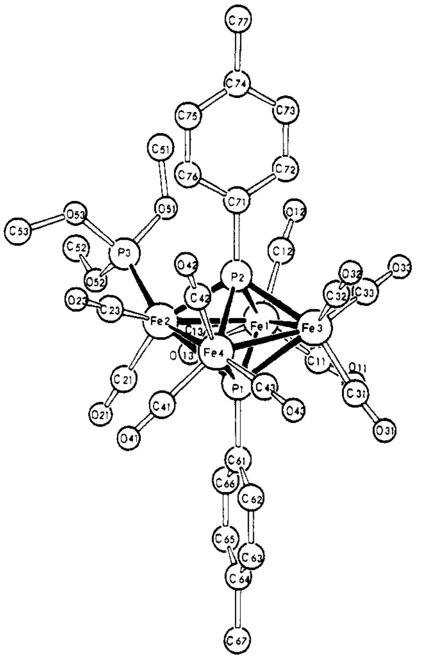

Figure 2. Molecular structure of $Fe_4(CO)_{11}(P\text{-}p\text{-}Tol)_2 \cdot P(OMe)_3$ (**4a**).

"loading" of these tetrairon clusters with PR_3 ligands seems possible.

The compositions and structures of **3a** and **4a**, two representative addition/elimination products, were proved by crystal structure analyses[10] (cf. Figures 1 and 2 and Table I). The overall similarity of both compounds is obvious. It corresponds to, but does not explain, their facile interconversion. The main difference between both structures lies in the metal atom arrangement and the CO orientations. The Fe_4 unit in **3a** is practically planar as evidenced by the nearly equidistant Fe–P1 and Fe–P2 bonds. Its geometry with one Fe–Fe bond shortened by a CO bridge closely resembles that of **1a**.[5] In contrast the Fe_4 unit in **4a** is significantly nonplanar with a folding angle along the Fe1···Fe4 diagonal of 163°. This difference seems to result from the optimization of the terminal ligand orientations. In **3a** each iron atom has one ligand in the tetrametal plane, one above and one below, whereas in **4a** the iron atoms alternatively have one ligand above and two ligands below the tetrametal plane and vice versa.

The structures of **3a** and **4a** suggest one explanation for the ease of their interconversions: the crowding of ligands in **4a** may favor CO elimination whereas the unsaturation of **3a** may favor CO addition. Another explanation is offered by electron bookkeeping: the clusters **2**, **4**, and **5** have the correct electron count for a Fe_4 quadrangle according to the 18-electron rule. The clusters **1** and **3**, however, have the correct electron count for a closo Fe_4P_2 unit according to Wade's rules.[11]

Table I. Important Bond Lengths (pm) and Angles (Deg) in 3a and 4a

	3a	4a
Fe1-Fe2	275.5 (3)	271.0 (2)
Fe1-Fe3	264.2 (3)	266.6 (2)
Fe2-Fe4	267.1 (3)	268.7 (2)
Fe3-Fe4	245.8 (3)	266.8 (2)
Fe1-P1	226.4 (5)	221.5 (2)
Fe2-P1	225.6 (5)	235.1 (2)
Fe3-P1	234.6 (5)	237.7 (2)
Fe4-P1	232.3 (5)	221.5 (3)
Fe1-P2	225.3 (5)	235.5 (2)
Fe2-P2	223.2 (5)	219.7 (2)
Fe3-P2	230.1 (5)	223.4 (2)
Fe4-P2	231.9 (5)	240.6 (2)
P1···P2	264.6 (8)	259.8 (3)
$Fe\text{-}C_{term.}$	175-184 (2)	175-184 (1)
$C_{term.}\text{-}O_{term.}$	110-116 (2)	111-116 (1)
Fe2-P3	217.0 (5)	218.4 (2)
P1-Fe-P2	69.4-72.2 (2)	68.3-69.6 (1)
Fe1-P1-Fe4	108.5 (2)	117.2 (1)
Fe2-P1-Fe3	107.6 (2)	105.5 (1)
Fe1-P2-Fe4	109.1 (2)	105.2 (1)
Fe2-P2-Fe3	110.0 (2)	116.4 (1)
$Fe\text{-}C_{term.}\text{-}O_{term.}$	177-178 (2)	174-180 (1)
Fe1-C13-O13	168 (2)	175 (1)
Fe2-C23-O23	171 (2)	178 (1)

The addition of substrates to metal–metal double bonds has only sparsely been investigated.[12] In cluster chemistry only the Os–Os double bond in $H_2Os_3(CO)_{10}$ is well studied.[2,4] Unsaturation, however, is more often found in clusters of nuclearity 4 and above. Some clusters, like the ones described here, offer the possibility for this type of basic cluster reaction which consists of the binding and activation of a substrate without opening up the cluster and without replacing other ligands. This reaction which also bears significance in the context of the cluster–surface analogy is another demonstration of the unique possibilities in cluster chemistry.

Acknowledgment. This work was supported by the Fonds der Chemischen Industrie and by the Rechenzentrum der Universität Freiburg.

Registry No. **1a**, 81534-74-9; **1b**, 81534-73-8; **1c**, 81534-72-7; **2a**, 81447-26-9; **2b**, 81456-90-8; **2c**, 81478-18-4; **3a**, 81534-75-0; **4a**, 81478-19-5; **4b**, 81478-20-8; **5a**, 81505-77-3.

Supplementary Material Available: Listings of the complete crystallographic details, all positional and anisotropic thermal parameters, all bond lengths and angles, and observed and calculated structure factors for both structures (30 pages). Ordering information is given on any current masthead page.

---

[10] Crystals of **3a** were obtained from toluene/hexane (1:2), those of **4a** from benzene/hexane (1:2). The crystal quality was checked by Weissenberg photographs; all other measurements were done on a Nonius CAD 4 diffractometer. **3a**: orthorhombic, space group $P2_12_12_1$, $Z = 4$, $a = 1289.0$ (8) pm, $b = 1478.5$ (4) pm, $c = 1819.7$ (3) pm. **4a**: triclinic, space group $P\bar{1}$, $a = 1300.0$ (2) pm, $b = 1506.9$ (3) pm, $c = 944.52$ (2) pm, $\alpha = 100.65$ (1)° $\beta = 107.35$ (1)°, $\gamma = 84.43°$. The structures were solved by Patterson and Fourier methods. Blocked matrix refinement (rigid body and isotropic for phenyl C and H atoms, anisotropic for all other nonhydrogen atoms) using unit weights resulted in R values of 0.045 for **3a** and 0.055 for **4a**. All details of the crystallographic work are documented in the supplementary material: Table A contains all crystallographic data; Tables B and C list all atomic parameters for **3a** and **4a**. Table D lists all bond lengths and angles for both compounds: Tables E and F give the F_o/F_c listings.

[11] Wade, K. *Adv. Inorg. Chem. Radiochem.* **1976**, *18*, 1.

[12] Cf. Curtis, M. D.; Messerle, L.; Fotinos, N. A.; Gerlach, R. F. In Chisholm, M. H. "Reactivity of Metal-Metal Bonds"; American Chemical Society: Washington, D.C. 1981; *ACS Symp. Ser.* No. 155, p 221.

Metal–Silicon Bonded Compounds. 16. The Structure of $(LiSiMe_3)_2 \cdot (Me_2NCH_2CH_2NMe_2)_3$, a Highly Reactive Silylating Agent

Berhan Teclé, William H. Ilsley, and John. P. Oliver*

Department of Chemistry, Wayne State University
Detroit, Michigan 48202

Received March 5, 1982

Summary: The structure of the highly reactive silylating agent, $(LiSiMe_3)_2 \cdot (Me_2NCH_2CH_2NMe_2)_3$, has been determined from single-crystal X-ray diffraction data collected

Table I. Experimental Data from the X-ray Diffraction Study on $(LiSiMe_2)_2 \cdot (Me_2NCH_2CH_2NMe_2)_3$

mol formula:	$Li_2Si_2N_6C_{24}H_{66}$
mol wt:	508.886
cryst syst:	monoclinic
space group:	$P2_1$
cell dimens at −22 °C	
a	8.625 (1) Å
b	24.893 (6) Å
c	9.526 (2) Å
β	115.41 (1)°
vol	1847.4 (6) $Å^3$
Z	2
d_{calcd}	0.916 g cm^{-3}
radiation:	Cu $K\bar{\alpha}$ (λ 1.541 78 $Å^{-1}$)
monochromator:	graphite crystal
reflctns measd:	$\bar{h},k,l$
2θ range:	0–115°
scan type:	$\theta-2\theta$
scan speed:	6°/min in 2θ
bkgd measurement:	stationary crystal–stationary counter at beginning and end of 2θ each for one-fourth of the time taken for the 2θ scan
std reflctns:	3($\bar{2}21$; $22\bar{2}$; $\bar{3}61$) measured every 97 reflections; no significant deviation from the mean was observed
unique data:	2539
unique data with $F^2 \geqslant 3.0\sigma(F_o^2)$:	2096
obsd coeff:	$\mu = 9.929\ cm^{-1}$
$F(000)$	572 electrons
R_F	0.061
R_{wF}	0.054

by counter methods at −22 °C. The compound was found to crystallize in the monoclinic system, space group $P2_1$, with unit-cell dimensions of a = 8.625 (1) Å, b = 24.893 (6) Å, c = 9.526 (2) Å, β = 115.41 (1)° d_{calcd} = 0.916 g cm^{-3}, V = 1847.4 (6) $Å^3$, and Z = 2.

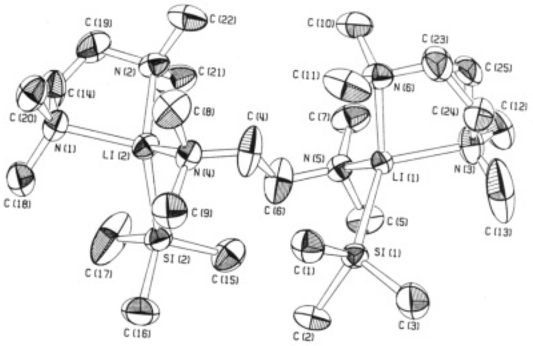

Figure 1. An ORTEP diagram for the molecular unit $(LiSiMe_3)_2 \cdot (TMEDA)_3$ with the atoms labeled. The atoms are represented by 25% thermal elipsoids. Positions 24 and 25 represent a disordered carbon atom, and in the refinement we assigned 50% occupancy factors.

Table II. Positional Parameters for the Nonhydrogen Atoms in $(LiSiMe_3)_2 \cdot (TMEDA)_3$

atom	x	y	z
Si(1)[a]	0.5613 (2)	0.7718	0.6713 (2)
Si(2)	0.1887 (3)	1.0267 (1)	0.2821 (3)
N(1)	0.4182 (8)	1.0205 (3)	−0.0008 (7)
N(2)	0.0965 (8)	0.9555 (3)	−0.1250 (7)
N(3)	0.1327 (9)	0.6814 (3)	0.4232 (11)
N(4)	0.4539 (8)	0.9001 (3)	0.2269 (7)
N(5)	0.1329 (7)	0.8226 (3)	0.3210 (7)
N(6)	0.3186 (9)	0.6996 (3)	0.2304 (7)
Li(1)	0.2810 (13)	0.7490 (5)	0.4064 (12)
Li(2)	0.2985 (15)	0.9678 (5)	0.1058 (13)
C(1)	0.7819 (10)	0.7690 (5)	0.6708 (11)
C(2)	0.5764 (12)	0.8435 (4)	0.7607 (10)
C(3)	0.6080 (15)	0.7300 (5)	0.8520 (12)
C(4)	0.3588 (12)	0.8571 (5)	0.2566 (15)
C(5)	0.0829 (11)	0.8354 (4)	0.4442 (10)
C(6)	0.2437 (14)	0.8675 (4)	0.3154 (15)
C(7)	−0.0240 (11)	0.8159 (5)	0.1746 (10)
C(8)	0.5383 (13)	0.8754 (5)	0.1372 (13)
C(9)	0.5857 (11)	0.9229 (5)	0.3688 (12)
C(10)	0.2306 (13)	0.7124 (4)	0.0647 (10)
C(11)	0.5039 (13)	0.6982 (6)	0.2777 (14)
C(12)	−0.0511 (12)	0.6818 (4)	0.3609 (13)
C(13)	0.1942 (18)	0.6659 (7)	0.5764 (23)
C(14)	0.2596 (14)	1.0373 (5)	−0.1319 (13)
C(15)	0.0198 (12)	1.0005 (4)	0.3420 (11)
C(16)	0.3577 (16)	1.0499 (6)	0.4743 (14)
C(17)	0.0818 (24)	1.0937 (5)	0.1916 (19)
C(18)	0.4933 (16)	1.0682 (5)	0.1003 (14)
C(19)	0.1523 (16)	0.9935 (5)	−0.2146 (10)
C(20)	0.5445 (12)	1.0016 (4)	−0.0531 (11)
C(21)	−0.0591 (12)	0.9728 (5)	−0.1212 (10)
C(22)	0.0720 (12)	0.9022 (5)	−0.1962 (11)
C(23)	0.2591 (18)	0.6461 (5)	0.2536 (14)
C(24)	0.2272 (31)	0.6391 (8)	0.3997 (31)
C(25)	0.1262 (35)	0.6458 (9)	0.2596 (33)

[a] y coordinate is fixed by crystallographic symmetry.

The greatly enhanced reactivity of organo- and silyllithium reagents, on the addition of a complexing agent such as *N,N,N′,N′*-tetramethylethylenediamine (TMEDA) has led to considerable speculation concerning the manner in which the base coordinates with the organometallic species.[1,2] It often is proposed that the active intermediate in solution is a simple coordinated species, LiR·(base)$_n$,[2] but the solid-state structural information obtained recently on a variety of simple alkyllithium derivatives, including $(LiMe)_4 \cdot (TMEDA)_2$,[3] $(LiPh)_2 \cdot (TMEDA)_2$,[4] and (bicyclo[1.1.0]butan-1-yl)lithium·TMEDA,[5] all contain fragments of the original organolithium aggregate which retain Li–C–Li multicentered electron-deficient bridge bonds. This indicates, at least in the solid state, that TMEDA is not a sufficiently strong coordinating agent to disrupt the lithium alkyl aggregate which lead to retention of the carbon-bridged systems.[6] Further, there is evidence from studies reported earlier[7] that addition of ether occurs in a stepwise fashion to the organolithium hexamers present in hydrocarbon solution with the species dissociating to tetramer only after two ether molecules have been attached.[7] Additional ether does not further degrade the tetramer which remains as the stable species in solutions.[8]

These observations and our recent report[9] that the trimethylsilyllithium·TMEDA complex, $(LiSiMe_3)_2 \cdot (TMEDA)_3$, shows both extreme and unusual reactivity led

---

(1) Wakefield, B. J. "The Chemistry of Organolithium Compounds"; Pergamon Press: Oxfor, 1974.

(2) Catala, J. M.; Clouet, G.; Brossas, J. *J. Organomet. Chem.* **1981**, *219*, 139 and references therein.

(3) Koster, H.; Thoennes, D.; Weiss, E. *J. Organomet. Chem. 1978*, *160*, 1.

(4) Thoennes, D.; Weiss, E. *Chem. Ber.* **1978**, *111*, 3157.

(5) Zerger, R. P.; Stucky, G. D. *J. Chem. Soc., Chem. Commun.* **1973**, 44.

(6) If the organic moiety readily forms a stable carbanion, i.e., triphenylmethyl etc., then the TMEDA complexes are best described as ion pairs in the solid state. See, for example: Patterman, S. P.; Karle, I. L.; Stucky, G. D. *J. Am. Chem. Soc.* **1970**, *92*, 1150. Brook, J. J.; Rhine, W.; Stucky, G. D. *Ibid.* **1972**, *94*, 7339. Brooks, J. J.; Stucky, G. D. *Ibid.* **1972**, *94*, 7333. Walczak, M.; Stucky, G. d. *Ibid.* **1976**, *98*, 5531.

(7) Extensive studies of base–organolithium interactions have been reported. See: Barlett, P. D.; Goebel, C. V.; Weber, W. P. *J. Am. Chem. Soc.* **1969**, *91*, 7425 and references therein.

(8) An excellent review of these studies has appeared: Brown, T. L. *Adv. Organomet. Chem.* **1965**, *3*, 365.

(9) Balasubramanian, R.; Oliver, J. P. *J. Organomet. Chem.* **1980**, *197*, C7.

Organometallics **1982,** *1,* 877–879

Table III. Selected Interatomic Distances (Å) and Angles (Deg) in (LiSiMe$_3$)$_2$·(TMEDA)$_3$

Bond Distances

Li(1)-Si(1)	2.70 (1)	Li(2)-Si(2)	2.69 (1)
Li(1)-N(3)	2.16 (1)	Li(2)-N(2)	2.16 (1)
Li(1)-N(5)	2.18 (1)	Li(2)-N(1)	2.17 (1)
Li(1)-N(6)	2.21 (1)	Li(2)-N(4)	2.15 (1)
Si(1)-C(1)	1.906 (8)	Si(2)-C(15)	1.89 (1)
Si(1)-C(2)	1.957 (9)	Si(2)-C(16)	1.88 (1)
Si(1)-C(3)	1.90 (1)	Si(2)-C(17)	1.92 (1)

Bond Angles

C(1)-Si(1)-C(3)	99.1 (5)	Li(1)-Si(1)-C(3)	119.2 (4)	Li(2)-Si(2)-C(16)	116.3 (5)
C(2)-Si(1)-C(3)	99.0 (5)	C(15)-Si(2)-C(16)	100.9 (4)	Li(2)-Si(2)-C(17)	115.0 (5)
C(1)-Si(1)-C(2)	98.9 (4)	C(16)-Si(2)-C(17)	101.0 (8)	N(1)-Li(2)-N(2)	87.0 (5)
Li(1)-Si(1)-C(1)	118.9 (4)	C(15)-Si(2)-C(17)	98.7 (5)	N(3)-Li(1)-N(6)	84.7 (5)
Li(1)-Si(1)-C(2)	117.2 (4)	Li(2)-Si(2)-C(15)	121.6 (4)		

us to determine its structure in the solid state by single-crystal X-ray diffraction techniques in an attempt to correlate the unusual reactivity of this species with its structural features.

The results of these studies are depicted in Figure 1 which shows an ORTEP diagram of the molecule with the atoms labeled. The features which are of major interest and importance are (1) the fact that there is no Li–Si–Li bridge bonding which shows that the hexameric aggregate, (LiSiMe$_3$)$_6$, has been completely destroyed, and (2) that the Li-Si bond distance is relatively long with a value of 2.70 Å even when compared to the average Li–Si distance of 2.68 Å, observed in the uncomplexed hexamer.[10] Further, examination of the bond angles around the silicon and lithium atoms (see Table I) shows that the C–Si–C angles are sharp with an average value of 100°. This should be compared with value observed in (LiSiMe$_3$)$_6$ of 103.3°,[10] of 102.9° in Mg(SiMe$_3$)$_2$·DME,[11] and 103.0° in Li$_2$Hg(SiMe$_3$)$_4$.[12] This further constraint, on the C–Si–C bond, may be interpreted in terms of additional negative charge being transferred to the SiMe$_3$ moiety and, along with the long Li–Si distance, account for both the high and unusual reactivity of this species.

Further work is currently in progress to determine the aggregation state of this species in solution and to determine if other silyl- or organolithium derivatives can be obtained which have both similar reactivity and structures.

(LiSiMe$_3$)$_6$ was prepared by the methods previously reported.[9] Approximately 1 g of the purified crystalline material was transferred, in an argon-filled drybox, to a reaction vessel which could be closed off and evacuated. This vessel was removed from the drybox, transferred to a vacuum system, and evacuated. Dry cyclopentane (~5 mL) was then distilled into the vessel followed by slow infusion of TMEDA. After several adjustments in concentration, crystals which appeared to be of suitable quality for X-ray study were obtained. Examination of a number of these crystals on the X-ray diffractometer, however, showed that they diffracted only weakly at room temperature. For that reason, data were collected at low temperature (−22 °C) using Cu K$\bar{\alpha}$ radiation on a Syntex P2$_1$ diffractometer. The crystal was found to be monoclinic and was ultimately assigned to the space group $P2_1$ on the basis of the systematic absences. The crystallographic data on the unit cell, and other pertinent data, are collected in Table I. The structure was solved by light atom techniques through the use of MULTAN[13] which gave positions for all of the nonhydrogen atoms except for a portion of one TMEDA unit. The structure was refined by standard techniques.[14] During the refinement, it was found that the TMEDA unit not originally located was disordered. This has been partially treated by assignment of 50% occupancy factors to two positions for one of the carbon atoms—represented by C(24) and C(25). This problem, along with thermal motion, led to initial difficulty in the solution of the structure and so far have prevented a better refinement of the structure.

Atomic coordinates for the nonhydrogen atoms are presented in Table II, and selected interatomic distances and angles are listed in Table III. Anisotropic thermal parameters, a complete listing of bond distances and bond angles, hydrogen positional parameters, and observed and calculated structure amplitudes are available.[15]

Acknowledgment. The work was supported by the National Science Foundation Grants CHE75-17217 and CHE80-16862. W.H.I. was supported by the Lubrizol Fellowship (1977–1978).

Registry No. (LiSiMe$_3$)$_2$·(Me$_2$NCH$_2$CH$_2$NMe$_2$)$_3$, 81583-50-8.

Supplementary Material Available: Tables containing anistropic thermal parameters, isotropic thermal parameters for hydrogen atoms, hydrogen positional parameters, all interatomic distances and angles, and observed and calculated structure amplitudes (20 pages). Ordering information is given on any current masthead page.

---

[10] Schaaf, T. F.; Butler, W.; Glick, M. D.; Oliver, J. P. *J. Am. Chem. Soc.* **1974,** *96,* 7593. Ilsley, W. H.; Schaaf, T. F.; Glick, M. D.; Oliver, J. P. *Ibid.* **1980,** *102,* 3769.

[11] Claggett, A. R.; Ilsley, W. H.; Anderson, T. J.; Glick, M. D.; Oliver, J. P. *J. Am. Chem. Soc.* **1977,** *99,* 1797.

[12] Ilsley, W. H.; Albright, M. J.; Anderson, T. J.; Glick, M. D.; Oliver, J. P. *Inorg. Chem.* **1980,** *19,* 3577.

[13] Germain, G.; Main, P.; Wolfson, M. M. *Acta Crystallogr., Sect. B* **1970,** *B26,* 274.

[14] Local versions of the following programs were used: (1) SYNCOR, Ws. Schmonsees' program for data reduction; (2) FORDAP, A. Zaltkin's Fourier program; (3) ORFLS and ORFFE, W. Buskin, K. Martin, and H. Levey's full matrix least-squares program and function error program; (4) ORTEP, C. K. Johnson's program for drawing crystal models. Scattering factors were taken from: Ibers, J. A.; Hamilton, W. C. "International Tables for X-ray Crystallography"; Kynock Press: Birmingham, England, 1974; Vol. IV.

[15] See the paragraph at the end of the paper regarding supplementary material.

Enhancement of ^{29}Si NMR Signals by Proton Polarization Transfer

Bradley J. Helmer and Robert West*

Department of Chemistry, University of Wisconsin
Madison, Wisconsin 53706

Received February 2, 1982

Summary: The application of polarization transfer via the INEPT pulse sequence to ^{29}Si NMR has been investigated for a wide variety of silicon compounds. The method was